SYNOPTIC-SCALE ANALYSIS OF TORNADO-PRODUCING TROPICAL CYCLONES ALONG THE GULF COAST

Ariel E. Cohen

NOAA/National Weather Service
Weather Forecast Office
Jackson, Mississippi

Abstract

Composite mean synoptic analyses are presented for seven different meteorological variables to distinguish between landfalling tropical cyclones along the coast of the Gulf of Mexico that are substantially tornadic (tropical cyclones that produce at least four tornadoes) and those that are not substantially tornadic (tropical cyclones that produce no more than one tornado). From 1985 to 2006, 15 landfalling tropical cyclones were identified as being substantially tornadic, while an additional 15 were identified as being non-substantially tornadic. These 30 tropical cyclones are considered separately amongst three sectors along the Gulf Coast in computing mean synoptic variables. Some findings for substantially tornadic tropical cyclones were: (1) the southeastern United States was broadly located within the right entrance region of an upper-level jet streak centered over the northeastern United States; (2) organized, large, and directionally-symmetric 850-hPa flow was maximized in the northeastern semicircle of the cyclonic envelope; (3) a distinct, organized, and symmetric mean sea level pressure pattern over the Gulf was associated with the tropical cyclones; (4) a strong 600-hPa relative humidity gradient was present in the northeastern semicircle of the cyclone; and (5) a dry intrusion was found in the eastern semicircle in some cases of substantially tornadic tropical cyclones. These commonalities associated with the substantially tornadic tropical cyclones were not found to be associated with the non-substantially tornadic tropical cyclones.

Corresponding Author: Ariel Cohen
National Weather Service, Jackson MS Weather Forecast Office
234 Weather Service Dr.
Flowood, MS 39232
e-mail: Ariel.Cohen@noaa.gov

Currently with the NOAA/NWS Storm Prediction Center, Norman, OK

1. Introduction

Numerous tropical cyclones (TCs) have tasked operational forecasters with a challenge to assess the tornado risk as they make landfall. Tornadoes associated with TCs are known to result in a major loss of life and property and account for 4% of the total deaths associated with TCs that make landfall in the United States (Rappaport 2000). However, some TCs have been responsible for more prolific tornado production than others. For example, in 2004, Hurricane Ivan made landfall along the United States Gulf Coast and was associated with an extraordinary 117 tornadoes across the United States, which were responsible for killing eight individuals (Stewart 2005). These tornadoes associated with landfalling TCs are receiving increasing attention within the severe convective storms research community for those reasons (e.g., McCaul 1991; Molinari and Vollaro 2008; and Rasmussen and Blanchard 1998). Previous and ongoing research has focused on the mesoscale environments associated with these tornadoes, with a particular focus on the distributions of instability and shear influencing these environments.

The majority of tornadoes associated with TCs have been found to occur in the right-front quadrant of the cyclones in an environment characterized by relatively weak instability and strong low-level vertical wind shear with the latter providing high values of low-level storm-relative helicity (Molinari and Vollaro 2008). As a result, mesocyclones within the severe local storms are typically shallow, with depths of around 3.5 km (Spratt et al. 1997). These mesocyclones are also transient and associated with weaker tornadoes. Most of the associated tornadoes are found within the outer rainbands of the TC, where limited diurnal heating between rain bands increases low-level instability. Previous work (i.e., Curtis 2004) has also identified that mid-level dry air entrainment within the 700-500-hPa layer supports tornado outbreaks (defined as producing at least 20 tornadoes) for landfalling TCs along the Atlantic and Gulf of Mexico Coasts. The present study focuses on the 600-hPa level for the analysis of relative humidity gradients and dry intrusions, which is representative of the 700-500-hPa layer identified in Curtis (2004) as being critical for analyzing tornadogenesis potential.

While our understanding of the mesoscale environment supporting tornadic TCs continues to grow, a major question remains somewhat unaddressed: what are the characteristics of the *synoptic-scale environment* associated with tornadoes produced by landfalling TCs? Belanger et al. (2009) took some of the first steps at investigating this problem. They created two regression models to explain the frequency of tornadoes associated with each Gulf of Mexico TC that makes landfall on the United States coastline. The inputs for these models include TC intensity indicated by the 10-m wind speed, horizontal size of the cyclone measured by the radius of the outermost closed isobar, recurvature of the TC, and middle-tropospheric specific humidity measured by the 500-hPa specific humidity gradient upon TC landfall. The formulation of their model that incorporates all four of the aforementioned variables (i.e., a regression model named *Recon*) was found to explain 70% of the actual tornado frequency associated with each landfall of a Gulf of Mexico TC during the period from 1998 to 2008.

While Belanger et al. (2009) specify meteorological parameters to forecast TC tornado frequency with an emphasis on synoptic-scale variables, and other studies document the mesoscale environment supporting TC tornadoes; the current study is intended to expand our qualitative understanding of the synoptic-scale environments favorable for producing tornadoes with landfalling TCs. This study explores a handful of variables related to those investigated by Belanger et al. (2009), as well as several other ones. More importantly, the present work provides spatial patterns of these variables, which is critical in pattern recognition, using reanalysis data provided by the National Centers for Environmental Prediction (NCEP)/National Centers for Atmospheric Research (NCAR) Reanalysis Project (Kalnay et al. 1996). Such a process provides the forecaster with useful hints as to what spatial distributions of variables are conducive for observed phenomena, including tornadoes associated with landfalling TCs.

The overall goal of this work is to provide operational forecasters with tools to better anticipate tornadic events associated with TCs and to distinguish those that are more likely to produce tornadoes from those that are less likely to produce tornadoes. Numerous synoptic charts are provided in this work from the reanalysis data to develop these tools, and forecasters are encouraged to employ synoptic pattern recognition in the forecast process when identifying the likelihood for a landfalling TC to produce a substantial number of tornadoes.

2. Data and Methodology

Table 1 provides a list of all substantially tornadic TCs (ST-TCs, those producing at least four tornadoes) investigated in this study, including the name of the TC, its intensity at landfall, and the date that was used for computing mean fields in the reanalysis. This date corresponds to the period within 24 hours of the greatest number of tornadoes occurring in association with the TC. For tornadoes occurring over longer durations, the selected date generally encompassed the initial reports

to represent preconditions supporting the tornado event. Tornado reports were queried using the *SeverePlot* program (Hart and Janish 2006), which includes reports from both digitized versions of the National Climatic Data Center (NCDC) publication *Storm Data* and the Storm Prediction Center online database (2010). While any report database contains uncertainty, it is assumed that they can reasonably determine whether a TC is a substantial tornado-producer or not. Table 1 also lists the degree of tornado production from each of the ST-TCs based on the aforementioned reports. These degrees are generalized into categories due to the uncertainties in the tornado reporting database and potential error in associating reports with a particular TC. Plan view maps of tornado reports associated with each of the TCs listed in Table 1 are provided in Fig. 1 based on output from the *SeverePlot* program.

A minimum of four tornadoes was required for a TC to be considered a ST-TC. This threshold is intended to discriminate between landfalling TC cases where there is a more substantial tornado risk from those which do not produce such a risk. While entirely arbitrary, the threshold of four tornadoes is used in this work as a proxy for substantial tornadic concern with a TC. The current study is intended to focus on a smaller subset of landfalling TCs that are more prolific tornado-producers, and after searching through severe weather databases, the number of four seemed to be an appropriate minimum threshold to separate the TCs associated with a greater frequency of reported tornadoes from those associated with a lower frequency. The strength of tornado played no role in the definition of a tornadic TC, as most of the tornadoes spawned by TCs are weak (F1 intensity or less) lending little opportunity for robust categorization of higher-intensity reports.

For a TC to be considered non-substantially tornadic (NST-TC), the TC had to have produced no more than one tornado. These cases are listed in Table 2. However, given the substantially-reduced visibilities with greater low-level moisture in TC environments, it is possible that tornadoes were produced in these cases but were not reported. The date of analysis listed in Table 2 for

Name	Intensity at Landfall (including hurricane category on the Saffir-Simpson Hurricane Wind Scale)	Date of Analysis	Region	Degree of Tornado Production
Jerry	Hurricane (1)	10/15/1989	WEST	A
Dean	T.S.	7/30/1995	WEST	A
Frances	T.S.	9/10/1998	WEST	B
Fay	T.S.	9/6/2002	WEST	B
Emily	Hurricane (3)	7/20/2005	WEST	B
Danny	Hurricane (1)	8/16/1985	CENTRAL	D
Juan	Hurricane (1)	10/28/1985	CENTRAL	B
Andrew	Hurricane (3)	8/25/1992	CENTRAL	D
Bill	T.S.	6/30/2003	CENTRAL	B
Rita	Hurricane (3)	9/24/2005	CENTRAL	D
Agnes	Hurricane (1)	6/18/1972	EAST	C
Florence	T.S.	9/10/1988	EAST	A
Isidore	T.S.	9/25/2002	EAST	A
Ivan (1st U.S. landfall)	Hurricane (3)	9/15/2004	EAST	D
Alberto	T.S.	6/12/2006	EAST	C

Table 1. ST-TC list providing the name, intensity at landfall, date of analysis, and region of landfall, along with degree of tornado production ("A" represents approximately 4-7 tornado reports, "B" represents 8 to 15 tornado reports, "C" represents 16 to 30 tornado reports, "D" represents at least 31 tornado reports).

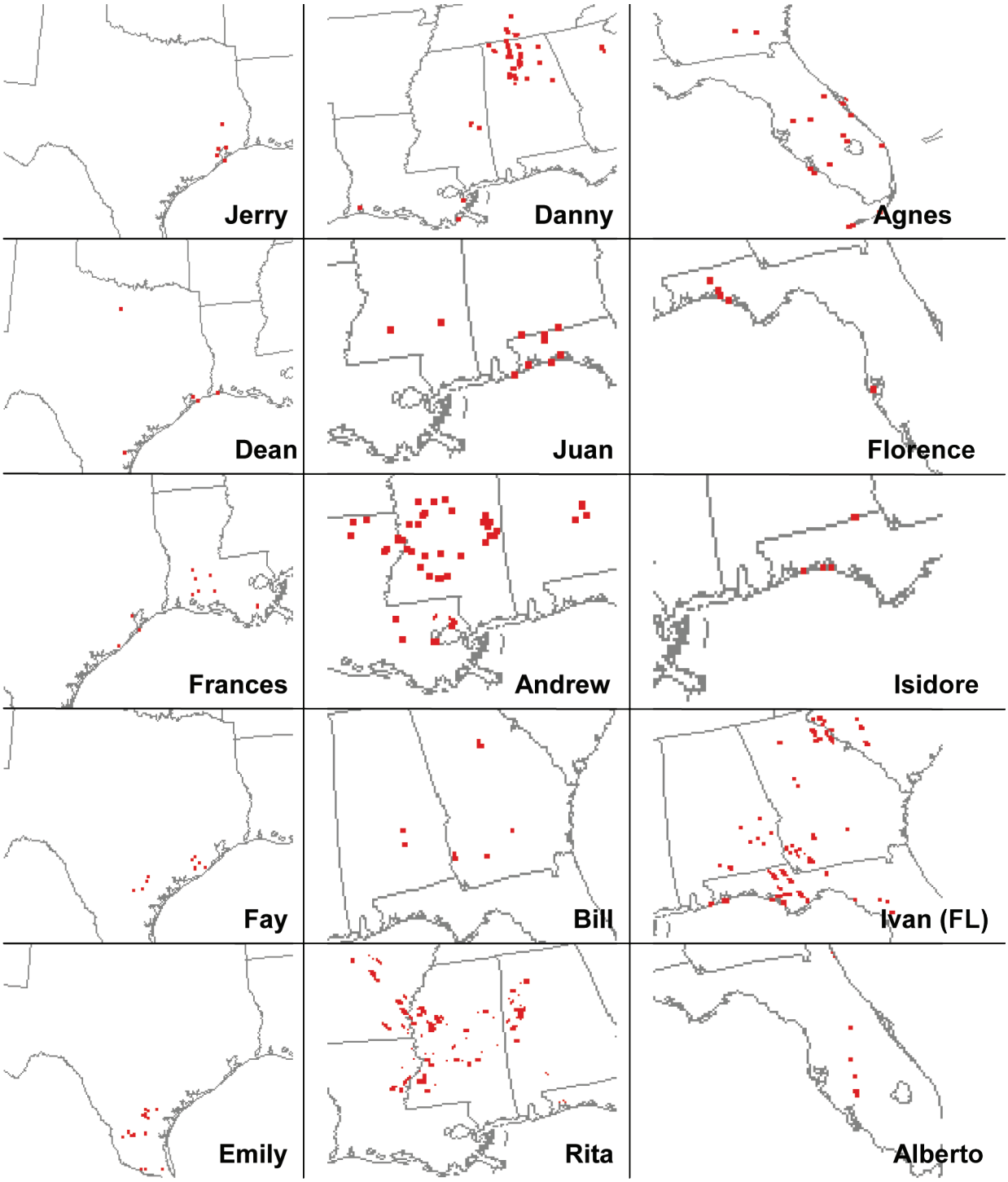

Fig. 1. Tornado reports (in red) associated with each of the TCs listed in Table 1.

NST-TCs corresponds to the period within 24 hours of the TC landfall and generally when the TC was over land for the longest time.

The tornado reports are evaluated regionally, such that the mean fields are studied separately for three regions along the Gulf Coast. The separation of cases into regions was chosen to reduce the amount of smoothing of mean fields across the entire Gulf region when averaging variables amongst the various cases. Figure 2 provides an approximate depiction of the spatial considerations for this study. For an ST-TC to be considered as being a member of a particular region, the majority of its associated tornadoes (i.e., tornadoes occurring within 360 km of the TC center and within one day of landfall) must have occurred in that region. The distance of 360 km seemed to most consistently capture the aerial extent of the synoptic-scale influence of the TCs considered in this study. The region for each NST-TC was where the one associated tornado occurred (i.e., tornado occurring within 360 km of the TC center and within one day of landfall). If the TC did not produce any reported tornadoes, the reported region corresponds to where the TC made landfall. The regions are also shown for each of the TCs listed in Tables 1 and 2. Each of the regions in Fig. 2 is represented by ellipses, and the regional centroid will often be referenced when describing distances from fundamental synoptic-scale features.

Name	Intensity at Landfall (including hurricane category on the Saffir-Simpson Hurricane Wind Scale)	Date of Analysis	Region
Chantal*	Hurricane (1)	8/1/1989	WEST
Arlene*	T.S.	6/21/1993	WEST
Beryl*	T.S.	8/15/2000	WEST
Bertha (TX)	T.D.	8/9/2002	WEST
Grace	T.S.	8/31/2003	WEST
Beryl	T.S.	8/9/1988	CENTRAL
Danny	Hurricane (1)	7/18/1997	CENTRAL
Ivan			
(3rd U.S. landfall)	T.S.	9/24/2004	CENTRAL
Matthew*	T.S.	10/9/2004	CENTRAL
Arlene	T.S.	6/11/2005	CENTRAL
Kate	Hurricane (2)	11/22/1985	EAST
Barry*	T.S.	8/6/2001	EAST
Henri*	T.D.	9/6/2003	EAST
Tammy*	T.D.	10/5/2005	EAST
Claudette*	T.S.	8/17/2009	EAST

Table 2. NST-TC list providing the name, intensity at landfall, date of analysis, and region of landfall (an asterisk indicates one tornado reported in association with the TC).

To develop the spatial analysis of potential predictors for tornadoes associated with landfalling Gulf of Mexico TCs, the present study uses the NCAR/NCEP reanalysis data. This reanalysis project uses the NCEP global spectral model, which includes 62 waves in a triangular truncation, as well as 28 vertical levels in sigma coordinates. The analysis scheme uses a three-dimensional variation (3DVAR) data assimilation scheme and assimilates numerous observational datasets (e.g., upper air sounding data including temperature and wind velocity, vertical temperature soundings from NOAA polar orbiters, satellite-derived winds from geostationary satellites, and surface observational data). The reanalysis was performed every six hours at synoptic times (0000 UTC, 0600 UTC, 1200 UTC, and 1800 UTC) on a 2.5° x 2.5° grid, and the average of the four hours of data from each day were used to create daily mean plots. These were then further averaged to create mean composite synoptic fields

Fig. 2. Graphical view of regional sectorization for tropical cyclone landfalls (the regions from left to right are west (a), central (b), and east (c)) (map backgrounds from Storm Prediction Center 2010).

for Gulf Coast landfalling TCs and to make comparisons between substantially tornadic TCs (ST-TCs) and non-substantially tornadic TCs (NST-TCs). Two individual ST-TC cases are also presented for additional illustration and analysis.

3. Discussion

a. Mean synoptic fields

1) 200-hPa flow

Figure 3 provides the mean 200-hPa wind vector fields across the United States with the left column indicating ST-TCs, and the right column containing NST-TCs. The top row (a) includes western region cases, the middle row (b) central region cases, and the bottom row (c) eastern region cases. This general format is followed for all remaining figures through Fig. 8. The most remarkable feature in Fig. 3 is the placement and strength of the 200-hPa jet streak relative to the Gulf Coast, which is particularly evident amongst the central and eastern region cases (b and c). For these two regions, the center of the jet streak is approximately 1100 km northeast of the regional centroids, which places the respective inland locations over the southeast United States in the favorable right entrance region of the jet streak. In this entrance region, the ascending branch of the ageostrophic circulation in the jet entrance region is driven by strong differential positive vorticity advection and upper level divergence. Note the southward placement of this jet streak in the tornado events as opposed to the non-tornado events. This pattern is not as apparent in the western region events (Fig. 3a). However, for the western region ST-TCs the weak jet maximum over Georgia, centered around 750 km east of the regional centroid, places portions of southern Louisiana in the right entrance region of this jet streak. In contrast, the corresponding jet maximum in the non-tornado events is oriented more north-to-south, and is displaced considerably to the east of the western region. The former jet pattern is somewhat reminiscent of an enhanced subtropical jet stream.

2) 850-hPa flow

In addition to considering the synoptic-scale environment unaffected by the TC, there are critical synoptic-scale mass and kinematic field responses to the TC, which, in turn, influence the propensity for a TC to be a substantial tornado-producer. While the variables that describe this response (e.g., 850-hPa flow field, mean sea level pressure, etc.) are certainly directly related to the TC itself, the influence of the TC on many mass and kinematic fields is typically expansive enough such that its spatial scale at least approaches the synoptic scale (i.e., several hundred to several thousand kilometers). Thus, a major influence governing the synoptic-scale environment in the vicinity of the TC tornadoes is the TC itself, and it is prudent to consider these larger-scale factors. More importantly, a distinction is being made here between the tornado, for which the associated flow fields are considered to be of "storm scale," and the TC, for which the associated flow fields are considered to be of a substantially larger scale. Arguably, in some of the smaller TCs, although the size of the cyclonic circulation and lower pressures and heights around the TC are small enough to be characterized as "mesoscale," these cases are being considered as "synoptic-scale" to highlight the larger-scale kinematic environment supportive of tornadoes.

The first of the variables which shows a definitive response to the presence of the TC is the 850-hPa flow field, as seen in Fig. 4. The most noticeable difference between the ST-TC and NST-TC cases is the considerably larger size and greater organization and directional symmetry of the 850-hPa storm-induced cyclonic wind field in the tornado events, in addition to the stronger 850-hPa flow in the northeast semicircle of the cyclonic envelope. Neither the strength nor organization of the 850-hPa flow is necessarily proportional to the size of the storm. Thus, the importance of cyclone size and organization associated with ST-TCs are important findings, consistent with those in Belanger et al. (2009), especially as more historical studies (e.g., Novlan and Gray 1974) have placed more of an emphasis on the strength of the storm as being a critical determining factor for tornadogenesis. These mean fields also show the strongest 850-hPa flow is found in the northeastern semicircle of the cyclone in a fixed reference frame. Since none of these calculations take into account the motion of any storm, this finding suggests that tornado risk identification on a storm-sector basis could be more efficiently done in a Cartesian-based reference frame than a storm-relative reference frame as suggested in Hill et al. (1966), and both can provide similar results. Additionally, comparison between the tornado reports in Fig. 1 and ST-TC tracks (not shown) suggests that most tornadoes occurred within the northeastern semicircle of the ST-TC tracks. The strength of the 850-hPa wind maximum is also important, with speeds of 10 to 14 m s^{-1} for the ST-TCs and speeds of 6 to 10 m s^{-1} for the NST-TCs.

Continued page 107

Fig. 3(a).

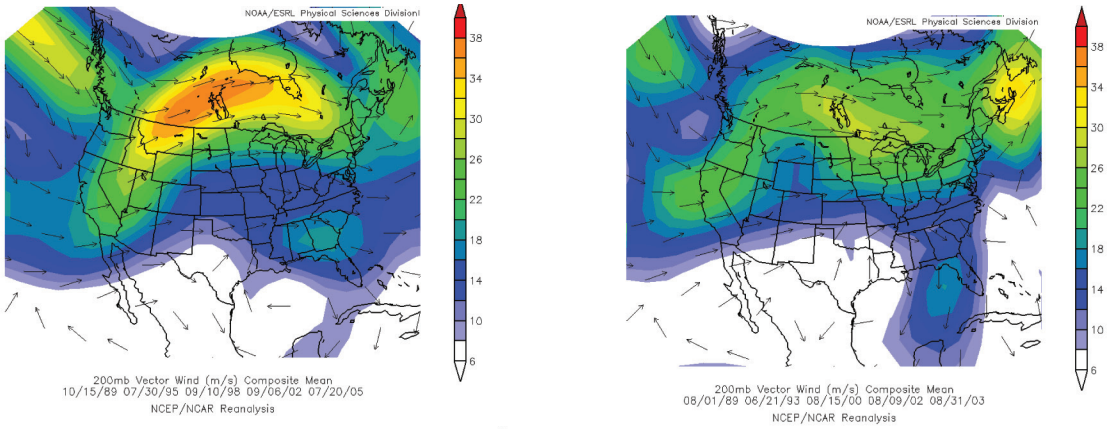

Fig. 3(b).

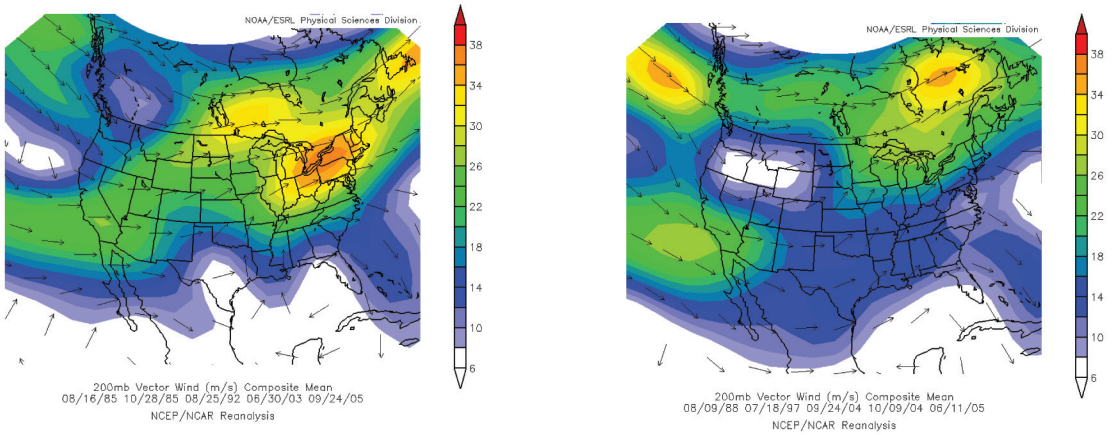

Fig. 3(c).

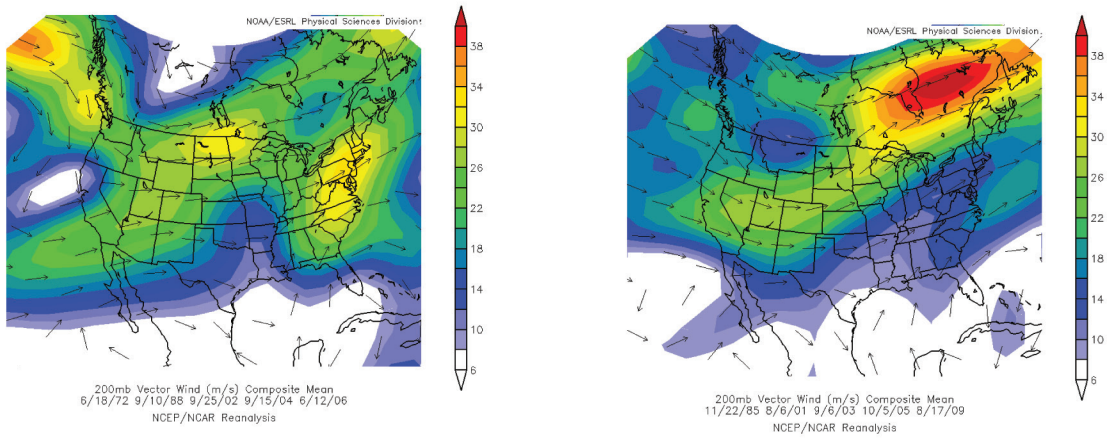

Fig. 3. Mean 200-hPa flow for ST-TCs (left column) and NST-TCs (right column) for west (a), central (b), and east (c) regions. Shading depicts wind speed in m s-1. Arrows indicate wind direction.

Fig. 4(a).

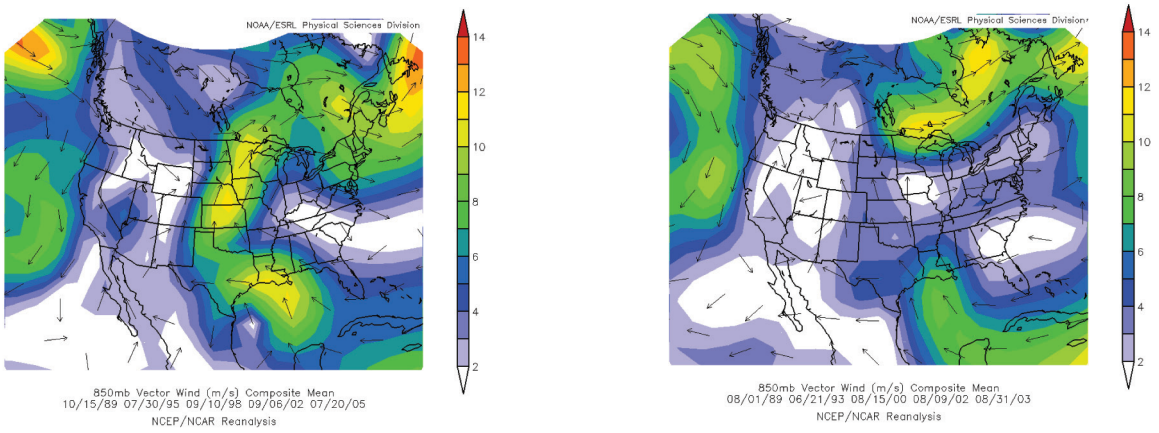

Fig. 4(b).

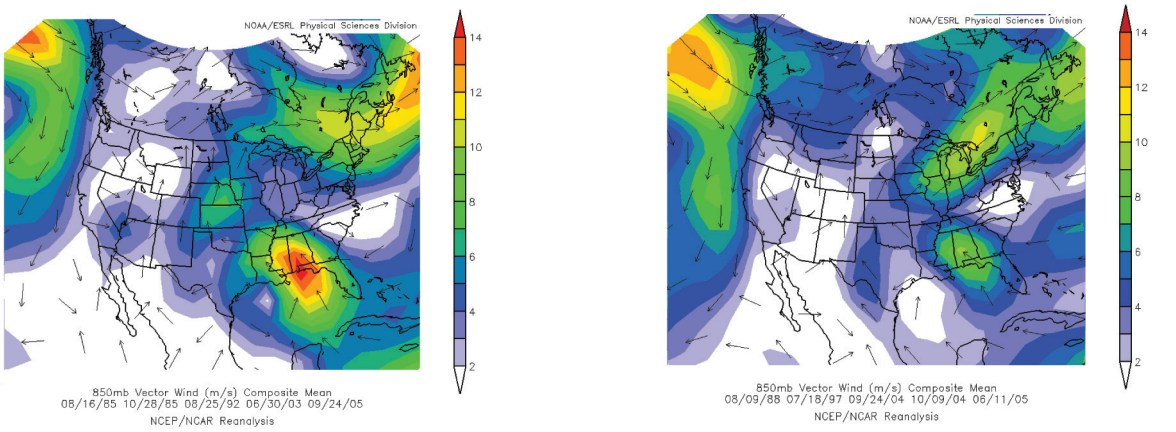

Fig. 4(c).

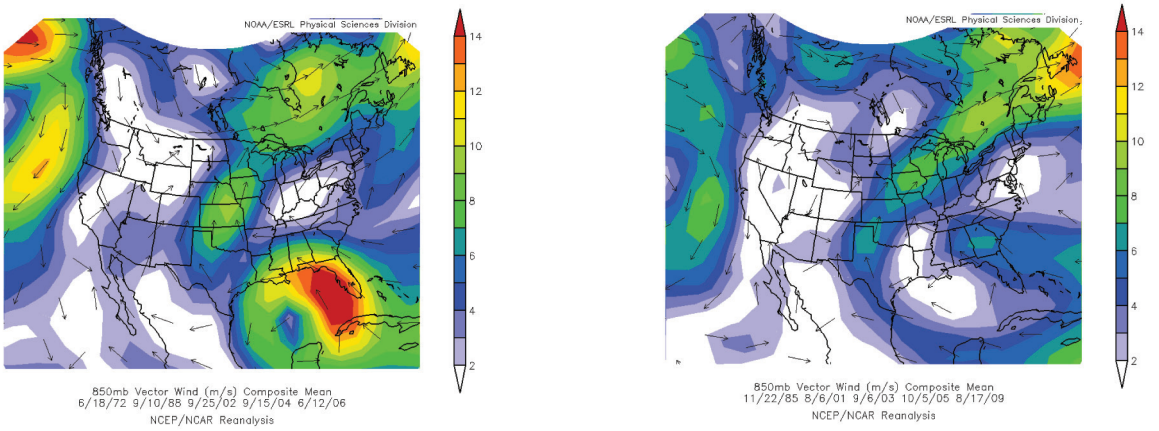

Fig. 4. Mean 850-hPa flow for ST-TCs (left column) and NST-TCs (right column) for west (a), central (b), and east (c) regions. Shading depicts wind speed in m s^{-1}. Arrows indicate wind direction.

3) 850-200-hPa bulk shear

The mean 850-200-hPa mean bulk shear vectors were also computed (not shown), and no substantial differences were found in this variable between the ST-TC and NST-TC environments. This suggests that large-scale, deep-layer shear plays an inconsequential role in enhancing the propensity of a TC to produce tornadoes. This is consistent with the finding that tornado-producing convection in TC environments has been found to be relatively shallow (e.g., Spratt et al. 1997) and thus unable to strengthen due to the presence of deep-layer shear.

4) Mean sea level pressure

The importance of system size and symmetry are also apparent in the mean sea level pressure (MSLP) fields, which are plotted in Fig. 5. Of particular note, the area of lower pressure associated with the ST-TCs appears to be well-defined and symmetric, as opposed to the broader trough in the NST-TCs. Also of note, mean minimum pressures below 1006 hPa are noted in each of the tornado events with the MSLP minima within 500 km of the regional centroids. The pressure gradient appears to be maximized over the northeast semicircle of the cyclone in the ST-TCs, approximately 500 km from the mean center of the TCs, which is also where the 850-hPa flow is also strongest. Once again, most of the tornado reports were found to occur in the northeastern semicircle of the ST-TCs.

As with the 850-hPa flow pattern, the larger-scale MSLP distribution is driven by the presence of the TC, which forces the kinematic field that can locally enhance the tornado potential with TCs. In particular, a simple gradient wind balance would suggest that the aforementioned gradient would drive a low-level flow with a more pronounced easterly component, where storm-relative helicity would be maximized due, in part, to low-level veering of flow. While helicity typically is considered to be a mesoscale variable, the synoptic-scale circulation plays a crucial role in locally enhancing these helicity values around the tornado. This maximization in storm-relative helicity is consistent with results discussed in Molinari and Vollaro (2008). This pressure gradient is substantially weaker in the NST-TCs, particularly in the west and central regions (Fig. 5a-b).

To further investigate the similar occurrences of larger TC size being associated with ST-TCs, as opposed to NST-TCs, the radius of the outermost closed isobar (ROCI) for each TC was computed from the reanalyses. In particular, the specific reanalysis hour (i.e., 00Z, 06Z, 12Z, or 18Z) closest to the tornado reports and landfall on the date of analysis listed in Tables 1 and 2, respectively, was used to compute the radii. For cases where the outermost closed isobar was more elliptical as opposed to circular, half the lengths of the minor axes were chosen to represent the radii. For these cases, the minor axes appeared to more consistently vary from TC to TC than the major axes, which is why the minor axes were chosen for the analysis of the ROCI. Amongst the ST-TCs, the average ROCI was around 390 km, whereas the average ROCI amongst the NST-TCs was around 230 km; and these differences highlight the spatial differences between the ST-TCs and NST-TCs.

In addition to investigating TC size, we can also further gauge the average strength amongst the ST-TCs and the NST-TCs. To do this, numerical ranks were assigned to the intensities for each of the TCs investigated as they made landfall (i.e., tropical depression assigned a rank of 1, tropical storm a rank of 2, category 1 hurricane a rank of 3, category 2 hurricane a rank of 4, and category 3 hurricane a rank of 4). Using the TC intensities listed in Tables 1 and 2, the mean rank amongst the ST-TCs is 3.1 and is 2.1 amongst the NST-TCs, thus highlighting the ST-TCs as being stronger than the NST-TCs upon landfall. Both the larger size and greater strength of the ST-TCs explain the ability for the NCAR/NCEP reanalysis fields to better resolve their circulations as seen in some of the figures. This, in itself, is an important finding, in that the large-scale influence of the NST-TCs is less pronounced than for ST-TCs.

5) 600-hPa relative humidity

Figure 6 displays the mean 600-hPa relative humidity fields, which reveal a spatially-broad, yet strong, horizontal gradient in mid-level moisture over the northwestern semicircle of the cyclone. The strongest gradient is found around 300 km northwest of the center of the 600-hPa TC-induced moisture maximum. In fact, this dry air is found to cyclonically envelop the storm intruding into its eastern semicircle in the central and, to a smaller degree, in the eastern region cases (Fig. 6b-c). This intrusion extends within 500 km of the center of the circulation. This process occurred with Hurricane Ivan and likely contributed to the numerous tornadoes reported in association with Ivan (Baker et al. 2009).

This gradient was also found by Curtis (2004), and supports the theory that the presence of a mid-level

Continued page 110

Fig. 5(a).

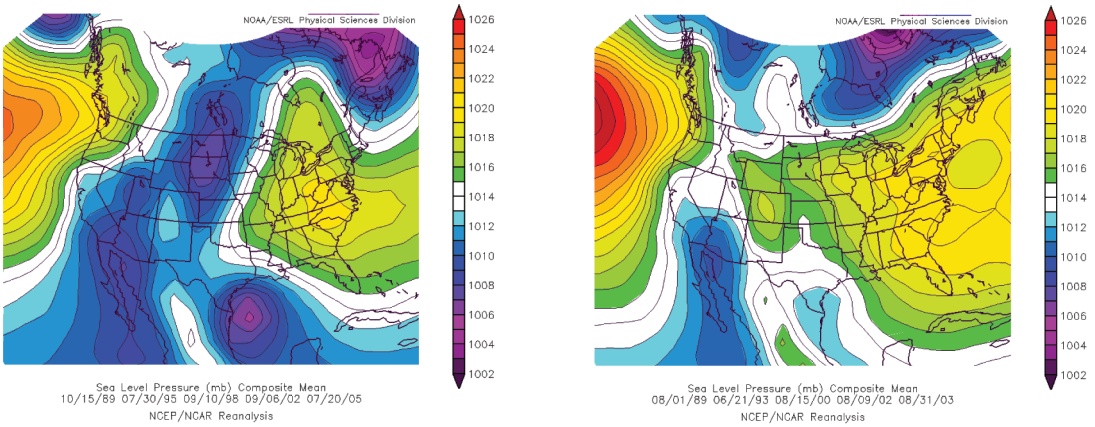

Fig. 5(b).

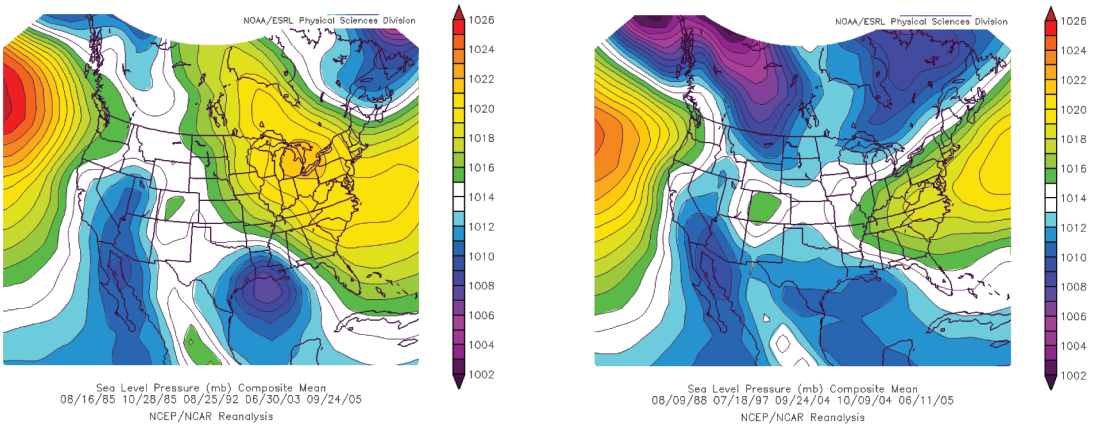

Fig. 5(c).

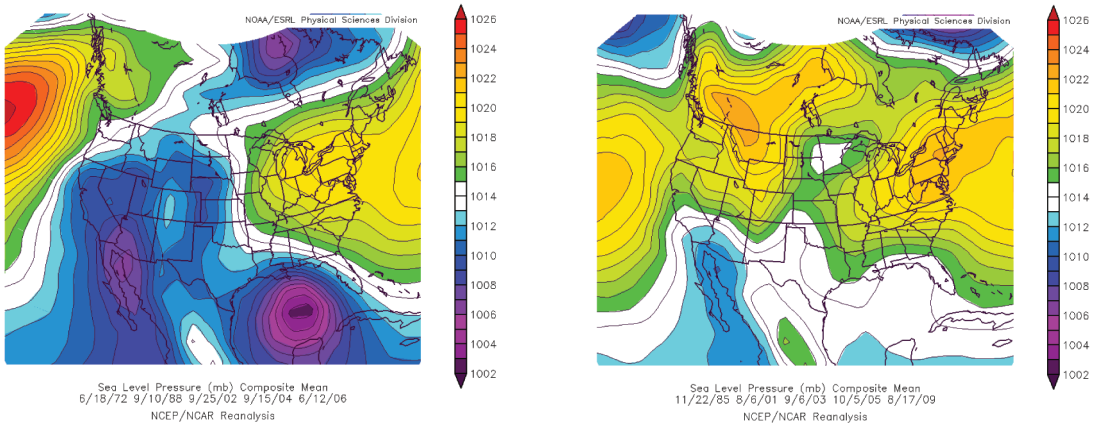

Fig. 5. Mean MSLP for ST-TCs (left column) and NST-TCs (right column) for west (a), central (b), and east (c) regions. Shading depicts MSLP in hPa.

Fig. 6(a).

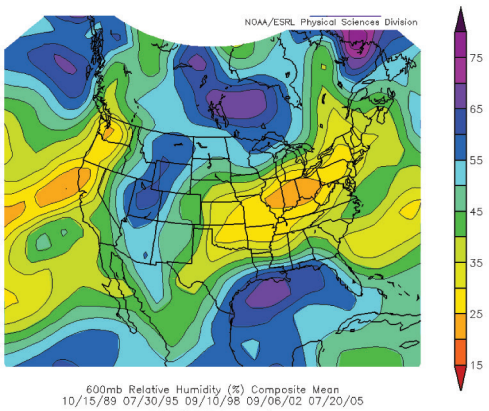

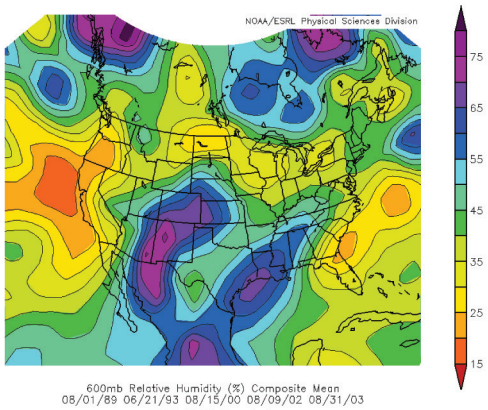

Fig. 6(b).

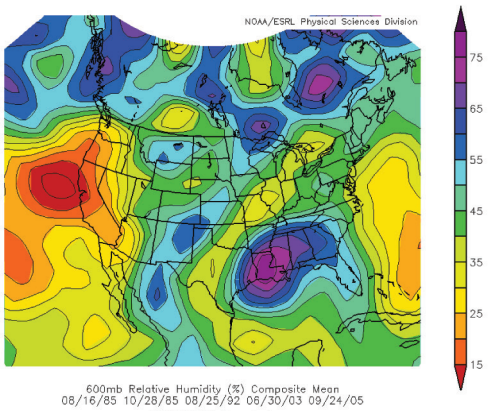

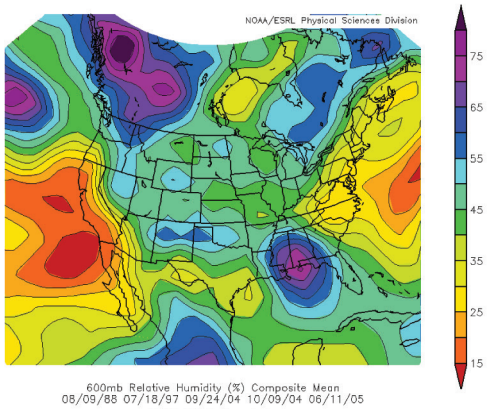

Fig. 6(c).

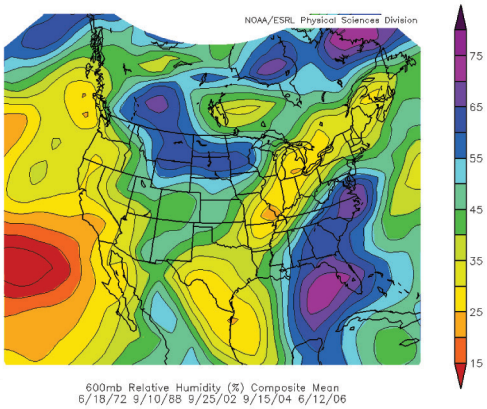

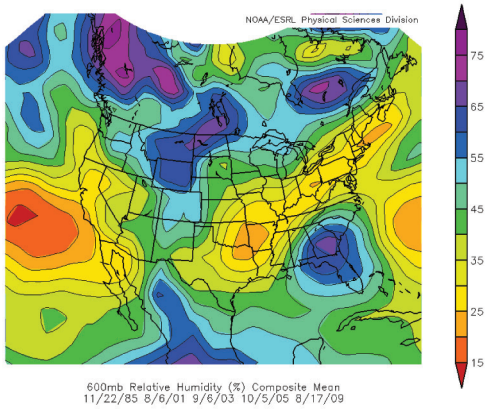

Fig. 6. Mean 600-hPa relative humidity for ST-TCs (left column) and NST-TCs (right column) for west (a), central (b), and east (c) regions. Shading depicts relative humidity in percent.

dry intrusion, evident in thermodynamic soundings, likely contributes to the development of cold pools in storms located in the outer rainbands. These cold pools can enhance the horizontal vorticity in the low levels, which can further deepen the lift in the presence of the unstable and particularly moist boundary layer of the outer rainbands. Also, the intrusion of mid-level dry air can increase low-level buoyancy by limiting the coverage of convection therefore increasing insolation. The presence of this dry air in the synoptic-scale environment can also be downscaled to smaller scales to explain local convective enhancements. In particular, it is speculated that the dry air could enhance the degree of potential instability and also enhance rear-flank downdrafts (RFDs) associated with supercells aiding in the tornadogenesis process. While the relative effects of evaporational cooling due to the presence of dry air and adiabatic warming of RFDs as they descend are not investigated in the present study, it is speculated that the dry, relatively denser air associated with ST-TCs enhance supercell RFDs and tornadogenesis through low-level vorticity stretching and transport, as well as low-level convergence.

Minimum relative humidities west of the strong gradient fall into the 25 to 35% range. Interestingly, this strong gradient is present in both the ST-TCs and NST-TCs for the eastern region (Fig. 6a). However, as in all tornado events, the size of the relative humidity enhancement associated with the TC appears to span a much larger region in space as compared to the NST-TCs. The relative humidity gradient is less defined in the NST-TCs, particularly for the central region events (Fig. 6b).

6) 500-hPa height field and 200-hPa temperature field

Mid- to upper-level mass and thermodynamic fields were investigated, and the 500-hPa height field and 200-hPa temperature fields are plotted in Figs. 7 and 8, respectively. Figure 7 reveals a typical synoptic pattern during hurricane season, with a mid-level trough over the western United States, with an upper ridge over the Plains. However, the depression in the 500-hPa heights in the vicinity of the TC is more pronounced in the ST-TCs with a closed 5825 geopotential meter contour in mean fields for the ST-TCs, and no closed contours for the non-tornado events. This feature is consistent with finding ST-TCs to be larger and stronger than NST-TCs. The positive upper-level temperature perturbation associated with the warm core nature of the ST-TCs is also more pronounced at 200 hPa than for NST's, again reflecting the stronger and larger ST-TCs as seen in Fig. 7. Both 500-hPa height minima and 200-hPa warm core centers are generally associated with the MSLP minima, reflecting the vertically-stacked nature of the landfalling TCs.

b. Individual cases

The NCEP/NCAR Reanalysis Project data were used to further investigate the synoptic environments associated with the approach of Hurricane Rita toward southeast Texas (analyses at 0000 UTC on 24 September 2005) and the approach of Tropical Storm Alberto toward Florida (analyses at 1800 UTC on 12 June 2006). Using the aforementioned criteria, both of these systems are considered ST-TCs. Figure 9 highlights the presence of the northeastern United States upper level jet, with associated upper level divergence in its right entrance region supporting synoptic-scale ascent and potential large-scale destabilization for the tornado events. While the strongest core winds are found to be relatively dislocated from the initial landfalling area, these winds are found to gradually trail off toward the south, which could still support sufficient upper level divergence to enhance convective activity.

Figure 10 illustrates the well-defined, broad relative humidity gradient at 600-hPa in the northwestern semicircle of Hurricane Rita (Fig. 10a), along with a dry intrusion into its eastern semicircle from the south. The dry intrusion is less pronounced, but still present for Tropical Storm Alberto (Fig. 10b); and the orientation of the relative humidity gradient is tilted quasi-zonally, but still present in the northern semicircle.

The 850-hPa pattern (Fig. 11) for both Hurricane Rita and Tropical Storm Alberto is fairly similar to that seen in the mean fields for ST-TCs with a relatively symmetric and well-organized height and wind field. However, some eccentricity is noted in the 850-hPa pattern for Tropical Storm Alberto, though both cases feature the strongest flow in the northeastern semicircle of the cyclonic envelope. *Continued page 112*

Fig. 7(a).

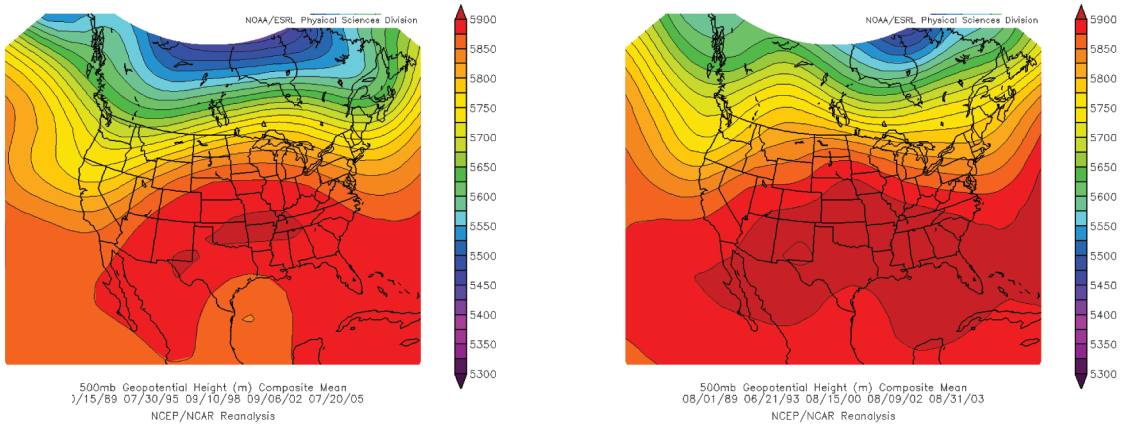

Fig. 7(b).

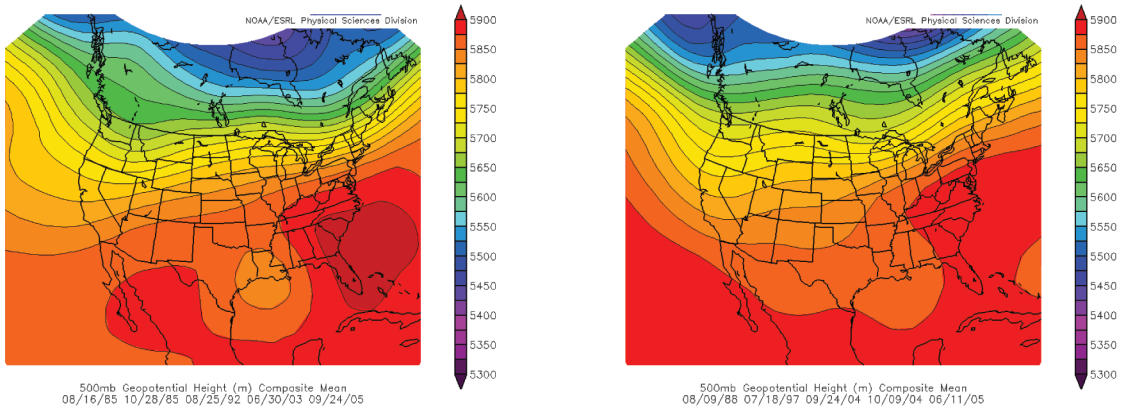

Fig. 7(c).

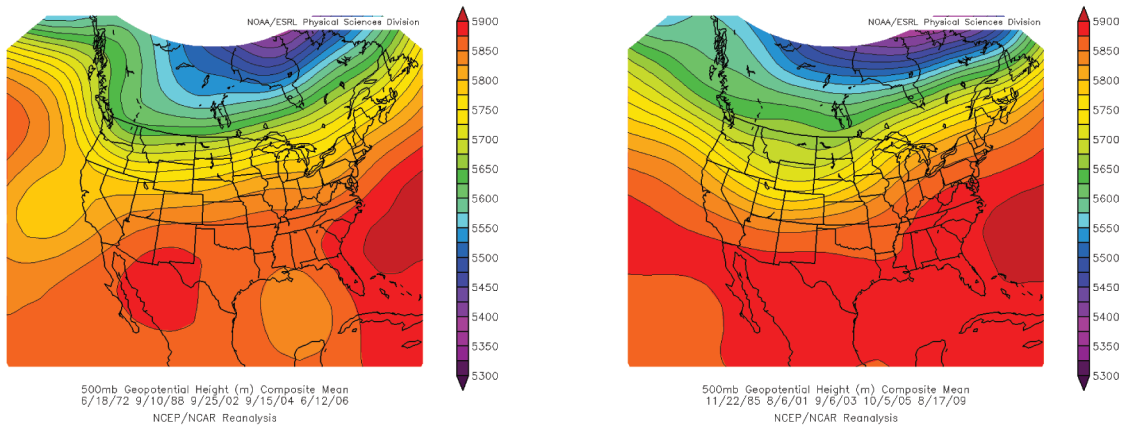

Fig. 7. Mean 500-hPa heights for ST-TCs (left column) and NST-TCs (right column) for west (a), central (b), and east (c) regions. Shading depicts height in geopotential meters.

Fig. 8(a).

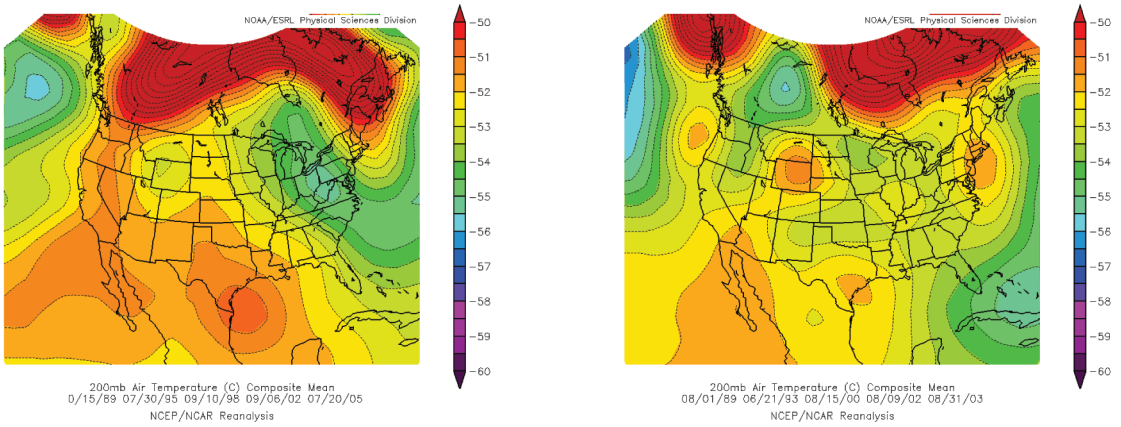

Fig. 8(b).

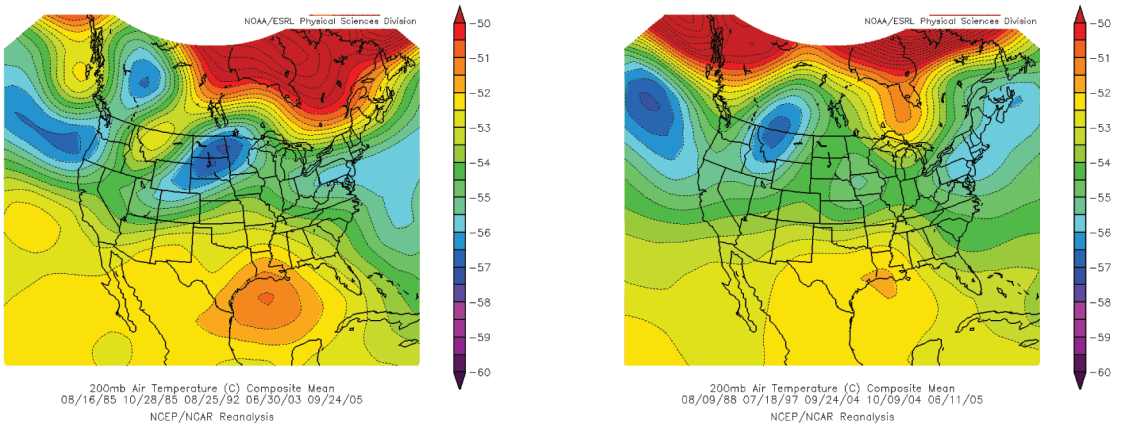

Fig. 8(c).

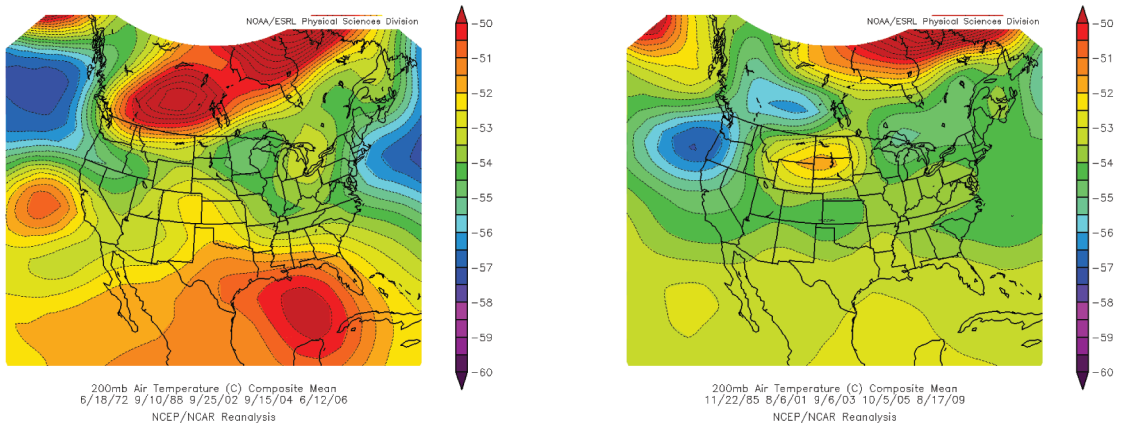

Fig. 8. Mean 200-hPa temperatures for ST-TCs (left column) and NST-TCs (right column) for west (a), central (b), and east (c) regions. Shading depicts temperature in degrees Celsius.

Conclusions

Much previous research has been performed to detail the buoyancy and shear distributions, as well as the mesoscale environments, supporting tornado outbreaks associated with landfalling tropical cyclones (TCs). The purpose of this study is to fit these mesoscale environments in the context of the synoptic-scale environment.

Fifteen landfalling TCs along the United States coast of the Gulf of Mexico from 1985 to 2006 were identified as substantially tornadic TCs (ST-TCs), producing at least four tornadoes, while an additional fifteen were identified as being non-substantially tornadic TCs (NST-TCs), producing no more than one tornado. Each of the fifteen cases was classified as occurring in one of three sectors adjacent to the Gulf coast, and several mean composite synoptic fields were computed to discriminate among the two event types for each sector.

Fig. 9(a).

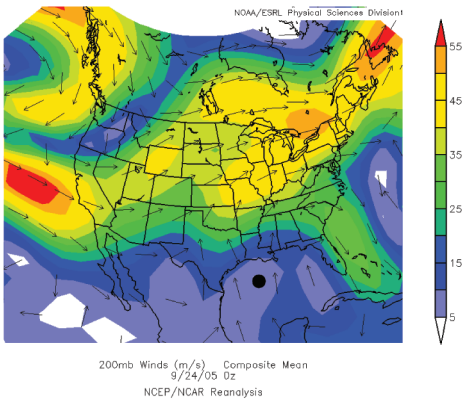

Fig. 9(b).

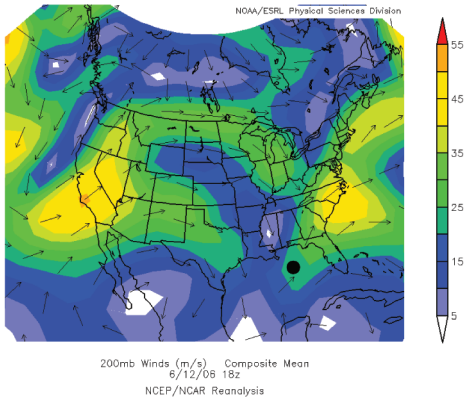

Fig. 9(c).

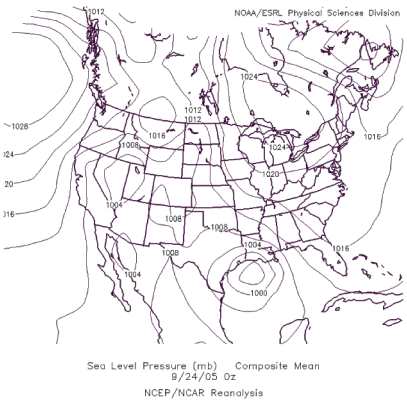

Fig. 9(d).

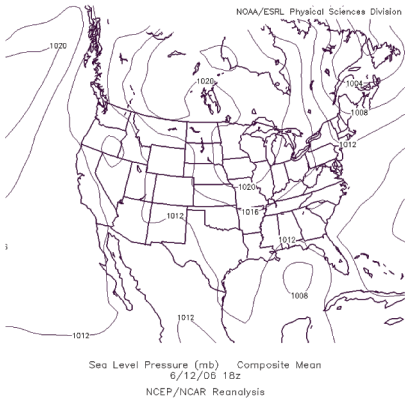

Fig. 9. Flow at 200 hPa (a and b) and MSLP (c and d) in the bottom row during the approach of Hurricane Rita (left column) and the approach of Tropical Storm Alberto (right column). The black dot depicts the approximate center of the surface circulation associated with the TC. Shading depicts wind speed in m s^{-1}. Arrows indicate wind direction.

Fig. 10(a).

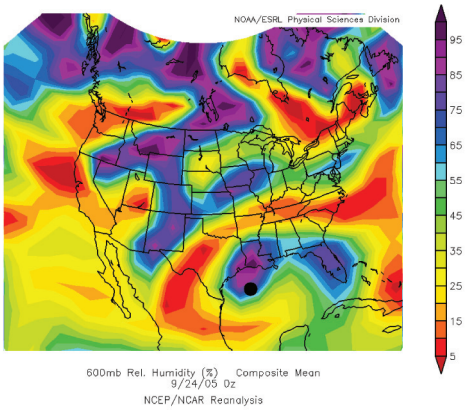

Fig. 10(b).

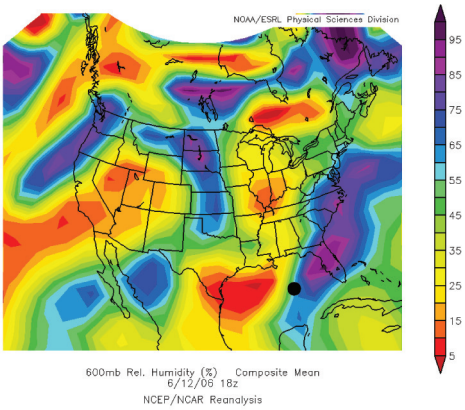

Fig. 10. Relative humidity at 600 hPa during the approach of Hurricane Rita (a) and the approach of Tropical Storm Alberto (b). The black dot depicts the approximate center of the surface circulation associated with the TC. Shading depicts relative humidity in percent.

Firstly, the right entrance region of an enhanced and 200-hPa jet streak centered over the northeastern United States was found to enhance the tornado potential with TCs across the southeastern United States. Any upper-level jet streak associated with the NST-TCs was substantially weaker. In the lower levels, the 850-hPa flow associated with the ST-TCs was found to be more organized, larger, directionally-symmetric, with the strongest flow found in the northeast semicircle of the associated cyclonic envelope. In this region, low-level storm-relative helicity is maximized, enhancing the tornadogenesis potential. Likewise, composite mean sea level pressure fields show a distinct, organized, and symmetric mean sea level pressure pattern over the Gulf

Fig. 11(a).

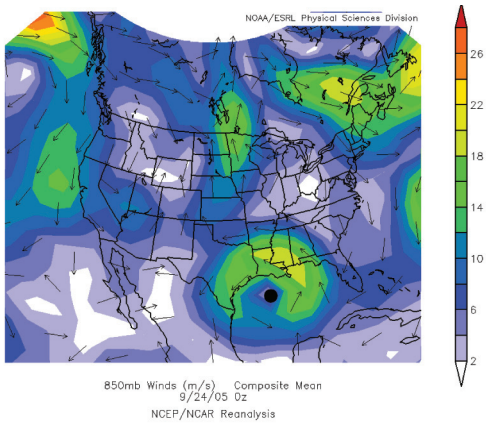

Fig. 11(b).

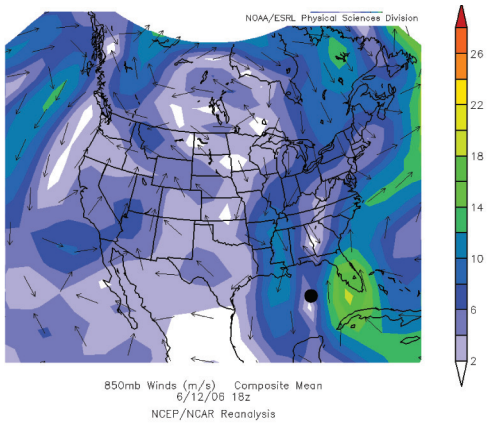

Fig. 11. Flow at 850 hPa during the approach of Hurricane Rita (a) and the approach of Tropical Storm Alberto (b). The black dot depicts the approximate center of the surface circulation associated with the TC. Shading depicts wind speed in m s^{-1}. Arrows indicate wind direction.

associated with the ST-TCs. This leaves the Gulf States in a tight pressure gradient supporting strong easterly gradient winds further enhancing low-level storm relative helicities. A much weaker pressure gradient is identified for the non-tornado events. Also, the ST-TCs were found to be larger and stronger than the NST-TCs.

Additionally, the presence of a 600-hPa relative humidity gradient is found over the northeastern semicircle of the cyclonic envelope. The dry air driving this gradient has been speculated to enhance low-level buoyancy in the vicinity of rain bands through mid-level dry air entrainment. ST-TCs are associated with deeper circulations extending above 500-hPa with evidence of stronger 200-hPa positive temperature perturbations. Individual case studies highlight these characteristics in the mean fields.

What makes the results in the present work particularly valuable to forecasters is that the features characterizing the synoptic-scale environments associated with ST-TCs were not found to exist in the NST-TC environments. Because of the differences between these environments, the results can provide guidance to operational forecasters in anticipating the potential for ST-TCs. Forecasters are encouraged to compare the synoptic-scale patterns presented in this study with observations and model forecasts of the patterns associated with land-falling TCs as a means for determining their potential to be substantially tornadic. Future work could develop quantitative guidance for evaluating TC tornado potential based on large-scale patterns; and this study provides clues for which variables could be investigated in developing such guidance.

Author

Ariel Cohen recently became a Mesoscale Assistant/ Fire Weather Forecaster at the Storm Prediction Center after working as a General Forecaster at the National Weather Service Weather Forecast Office (WFO) in Jackson, Miss., since August 2009. At the WFO Jackson, he was involved with numerous projects to enhance the Graphical Forecast Editor for a wide array of local interests including convective, fire, fog, and lake weather forecasts. He was also involved in a handful of local projects and case studies with an emphasis on severe convection. Prior to working in Jackson, Ariel was a Surface Analyst and Marine Forecaster with the Tropical Analysis and Forecast Branch of the National Hurricane Center in Miami, Florida. There, he worked with a team that developed the Graphical Forecast Editor for national center marine domains and led research initiatives in gale wind forecasting in the Gulf of California. Prior to moving to Miami, Ariel started his National Weather Service career as a General Forecaster at the Weather Forecast Office in Great Falls, Montana in 2007. After receiving his B.S. degree in Atmospheric Sciences from The Ohio State University in 2006, he received his M.S. degree in Meteorology from the University of Oklahoma in 2008 where he performed research with the National Severe Storms Laboratory in storm electrification modeling.

References

Baker, A. K., Paker, M. D., and Eastin M. D., 2009: Environmental ingredients for supercells and tornadoes within Hurricane Ivan. *Wea. Forecasting*, 24, 223-244.

Belanger, J. I., J. A. Curry, and C. D. Hoyos, 2009: Variability in tornado frequency associated with U.S. landfalling tropical cyclones. *Geophys. Res. Lett.*, 36, L17805.

Curtis, L., 2004: Midlevel dry intrusions as a factor in tornado outbreaks associated with landfalling tropical cyclones from the Atlantic and Gulf of Mexico. *Wea. Forecasting*, 19, 411–427.

Hart, J. A., and P. R. Janish, cited 2006: SeverePlot: Historical severe weather report database. Version 2.0. Storm Prediction Center, Norman, OK. [Available online at http://www.spc.noaa.gov/software/svplot2/]

Hill, E., W. Malkin, and W. Schulz, 1966: Tornadoes associated with cyclones of tropical origin-practical features. *J. Appl. Meteor.*, 5, 745–763.

Kalnay, E., M. Kanamitsu, R. Kistler, W. Collins, D. Deaven, L. Gandin, M. Iredell, S. Saha, G. White, J. Woollen, Y. Zhu, A. Leetmaa, R. Reynolds, M. Chelliah, W. Ebisuzaki, W. Higgins, J. Janowiak, K. C. Mo, C. Ropelewski, J. Wang, R. Jenne, and D. Joseph, 1996: The NCEP/NCAR 40-year reanalysis project. *Bull. Amer. Meteor. Soc.*, 77, 437–471.

McCaul, E. W., 1991: Buoyancy and shear characteristics of hurricane-tornado environments. *Mon. Wea. Rev.*, 119, 1954–1978.

Molinari, J., and D. Vollaro, 2008: Extreme helicity and intense convective towers in hurricane Bonnie. *Mon. Wea. Rev.*, 136, 4355–4372.

Novlan, D. J., and W. M. Gray, 1974: Hurricane-spawned tornadoes. *Mon. Wea. Rev.*, 102, 476–488.

Rappaport, E. N., 2000: Loss of life in the United States associated with recent Atlantic tropical cyclones. *Bull. Am. Meteorol. Soc.*, 81, 2065–2073.

Rasmussen, E. N., and D. O. Blanchard, 1998: A baseline climatology of sounding-derived supercell and tornado forecast parameters. *Wea. Forecasting*, 13, 1148–1164.

Spratt, S. M., D. W. Sharp, P. Welsh, A. Sandrik, F. Alsheimer, and C. Paxton, 1997: A WSR-88D assessment of tropical cyclone outer rainband tornadoes. *Wea. Forecasting*, **12**, 479–501.

Stewart, S., cited 2005: Tropical Cyclone Report, Hurricane Ivan, 2-24 September, 2004. National Hurricane Center. [Available online at http://www.nhc.noaa.gov/pdf/TCR-AL092004_Ivan.pdf]

Storm Prediction Center, cited 2010. [Available online at http://www.spc.noaa.gov.]

Acknowledgments

I thank the staff of the National Weather Service in Jackson, Mississippi, and at the National Hurricane Center in Miami, Florida, for numerous discussions and motivation to further study synoptic environments associated with land-falling TCs along the Gulf of Mexico Coast, particularly Mr. Alan Gerard and Mr. Greg Garrett of the National Weather Service Jackson, Mississippi; Dr. Christopher Landsea of the National Hurricane Center in Miami, Florida; and Mr. Russell Pfost, formerly of the National Weather Service in Miami, Florida. I also thank Laura Kanofsky of the National Weather Service in St. Louis, Missouri, for her review of this work, along with all editors for their input in bettering this work. All of this feedback greatly improved the quality of this work.